Absolute cross sections for electron-impact single ionization of Kr^{4+}, Kr^{5+}, and Kr^{7+} ions

M. E. Bannister
Physics Division, Oak Ridge National Laboratory, Oak Ridge, Tennessee 37831-6372

X. Q. Guo* and T. M. Kojima†
Joint Institute for Laboratory Astrophysics of the University of Colorado and the National Institute of Standards and Technology, Boulder, Colorado 80309-0440

(Received 20 December 1993)

Absolute total cross sections for electron-impact single ionization of Kr^{4+}, Kr^{5+}, and Kr^{7+} ions have been measured using a crossed-beams technique from below threshold to 500, 400, and 500 eV, respectively, with absolute uncertainties of 12% or less. The measured cross sections are in good agreement with distorted-wave calculations and show significant contributions from excitation autoionization. Nonzero cross sections below threshold for the Kr^{4+} and Kr^{5+} ions suggest the presence of metastable ions in those two species that were extracted from an electron-cyclotron-resonance ion source. Such evidence of metastable ions was not found in the case of the Kr^{7+} ion measurment.

PACS number(s): 34.80.Kw

I. INTRODUCTION

Electron-impact ionization of ions is an important atomic process in laboratory and astrophysical plasmas. Accurate cross sections and rate coefficients are required for modeling and diagnosing these plasmas. Much work has been done on electron-impact ionization of ions [1], but cross sections are lacking for several key ions of interest to fusion researchers [2]. In particular, cross sections for ionization and excitation of krypton ions by electrons are critical for understanding tokamak plasmas into which krypton has been injected to facilitate core ion temperature measurements [3]. Highly ionized krypton ions will be dominant in the core plasma, but moderate to low charge states will be abundant in the edge plasma.

In this paper, we report absolute total cross sections for electron-impact single ionization of Kr^{4+}, Kr^{5+}, and Kr^{7+} ions, with outer shell ground configurations of $4s^24p^2$, $4s^24p$, and $4s$, respectively. The only previously published cross sections for ionization of multicharged krypton ions were for single ionization of Kr^{2+} [4–7], Kr^{3+} [4,5,7,8], and Kr^{8+} [9], for double ionization of Kr^{q+} ($q=2,3,4$) [10,11], and for triple ionization of Kr^{2+} [11]. Cross sections for single ionization of Zn^+, isoelectronic with Kr^{7+}, have also been reported [12]. Since it is not practical to measure the ionization cross sections for all 36 charge states of krypton ions, we have concentrated on a few ions for which indirect ionization processes should be significant [13]. Measurement of the ionization cross sections for Kr^{6+} was also attempted but found not to be possible because of extremely high ion backgrounds encountered for that system, presumably due to autoionizing metastables in the ion beam.

The ionization cross sections reported here were measured using the Oak Ridge National Laboratory (ORNL) electron-ion crossed-beams apparatus. The results will be compared to distorted-wave calculations for direct and total ionization given in the following paper [14].

II. EXPERIMENT

The experimental method and ORNL crossed-beams apparatus have been described in detail elsewhere [15], so only a brief overview will be presented here. However, a recent modification to the apparatus, changing from a magnetically confined electron gun [16] to an electrostatically confined one, will be discussed in some detail. A schematic drawing of the apparatus is shown in Fig. 1.

A. Ion and electron beams

Krypton ions are extracted from the recently upgraded ORNL electron-cyclotron-resonance ion source at 10 kV and analyzed by a 90° magnetic analyzer. After traversing a few meters of beamline and optics, the ion beam is "purified" by a 90° parallel-plate analyzer before entering the collision volume where it is crossed by the electron beam. Downstream of the collision volume, a double-focusing magnet deflects the product $Kr^{(q+1)+}$ ions by 90° dispersing them from the primary Kr^{q+} ion beam. The product ions are then deflected through 90° out of the plane of the magnetic deflection and onto a channel electron multiplier. The primary krypton ions are collected in a movable Faraday cup shown in Fig. 1. The position of this cup depends on the charge ratio of the primary and product ions.

The electron gun employed uses electrostatic confinement of the beam instead of the previously used

*Present address: Chemical and Analytical Sciences Division, Oak Ridge National Laboratory, Oak Ridge, TN 37831.
†Present address: Atomic Physics Laboratory, Institute of Physical and Chemical Research, Saitama, Japan.

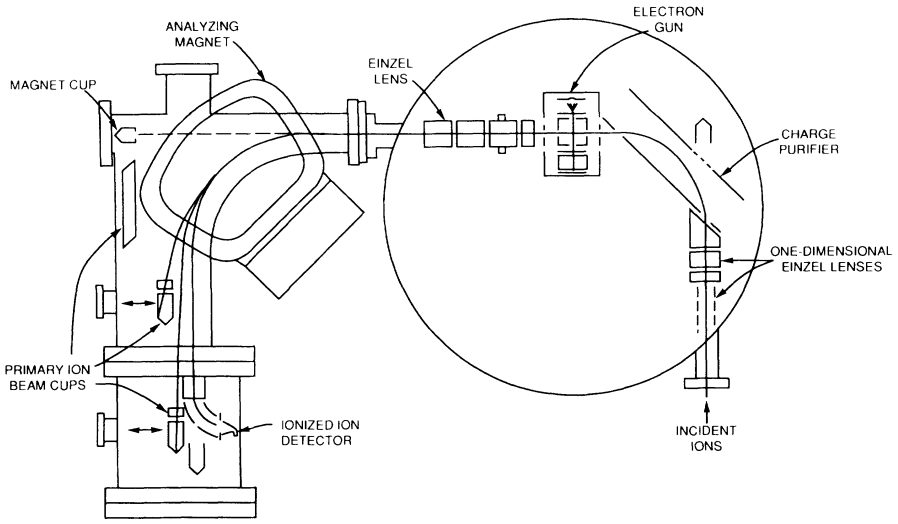

FIG. 1. Electron-ion crossed-beams experimental apparatus. See text for explanation.

magnetic confinement scheme [16]. The new electron gun is expected to have a higher energy resolution than the previous one, which will facilitate measurements involving higher charge states, and will make possible future studies of ejected electrons. Details of this electron gun have been published [17]. The gun, collision volume, and collector are magnetically shielded so that fields in these regions are less than 40 mG. After passing through the collision volume, the electrons are driven by a transverse electric field onto a collector plate covered with metal "honeycomb." Electron current to the box surrounding the collision volume is always less than 1% of the total electron current. However, at electron energies less than 150 eV, a fraction of the electron current passing through the collision volume strikes a shielding electrode between the collision box and the collector. This fraction ranges from less than 2% at 125 eV to about 20% at 40 eV. Some of the electrons striking this collector shield pass through the ion beam; this was verified by beam profile measurements using the current to the shield. The measured electron current is the sum of the currents to the collector and the shield. During data taking, the electron beam is chopped at 50 Hz by applying a square-wave voltage to the extraction electrode of the gun.

The profiles of the electron and ion beams in the direc-

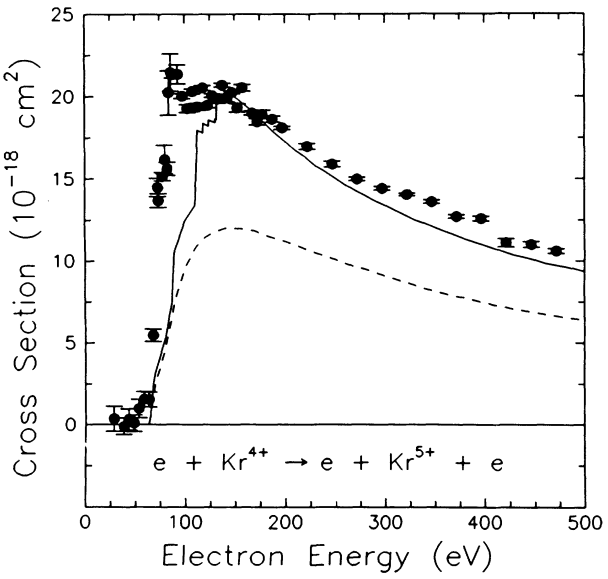

FIG. 2. Absolute cross sections as a function of electron-impact energy for single ionization of Kr^{4+}. The present experimental results are indicated by the solid circles with relative uncertainties at the one-standard-deviation level. The curves are results of configuration-average distorted-wave calculations: dotted curve, direct ionization only; solid curve, direct ionization plus excitation-autoionization (Ref. [14]).

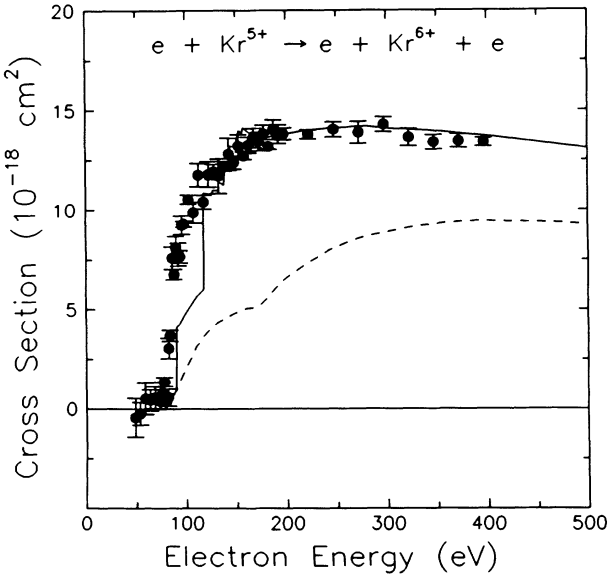

FIG. 3. Absolute cross sections as a function of electron-impact energy for single ionization of Kr^{5+}. The present experimental results are indicated by the solid circles with relative uncertainties at the one-standard-deviation level. The curves are results of configuration-average distorted-wave calculations: dotted curve, direct ionization only; solid curve, direct ionization plus excitation-autoionization (Ref. [14]).

tion perpendicular to both beams are measured using an L-shaped beam probe with coplanar slits, each 0.15 mm wide. A stepping motor drives the probe in accurate 0.15-mm steps over 1.27 cm. The current profiles are then integrated numerically to yield the "form factor," a geometric quantity quantifying the overlap of the two beams.

The absolute cross section is determined [18] from the measurements by

$$\sigma(E)=\frac{R}{I_e I_i}\frac{qe^2 v_e v_i}{\sqrt{v_e^2+v_i^2}}\frac{F}{D}\ , \tag{1}$$

where $\sigma(E)$ is the absolute cross section at the center-of-

TABLE I. Absolute total cross sections for electron-impact single ionization of Kr^{4+}. The relative uncertainties are at the one-standard-deviation level; the absolute uncertainties (given in parentheses) are at a high confidence level corresponding to 90% confidence for the relative uncertainties.

E (eV)	σ (10^{-18} cm^2)	
28.5	0.35±0.77	(1.30)
38.6	−0.10±0.52	(0.88)
43.4	0.30±0.66	(1.12)
48.7	0.08±0.50	(0.85)
53.4	0.98±0.56	(0.96)
58.7	1.56±0.48	(0.83)
63.4	1.54±0.46	(0.79)
68.0	5.48±0.38	(0.79)
72.9	14.49±0.56	(1.52)
73.5	13.69±0.42	(1.32)
77.8	15.14±0.26	(1.30)
80.0	16.19±0.87	(1.98)
82.5	15.62±0.41	(1.44)
83.8	20.24±1.35	(2.82)
86.0	21.47±1.13	(2.59)
87.7	21.34±0.21	(1.77)
92.7	21.36±0.58	(1.99)
97.6	20.03±0.15	(1.64)
102.5	19.29±0.23	(1.61)
107.6	20.32±0.14	(1.66)
112.6	19.39±0.22	(1.61)
117.6	20.54±0.14	(1.68)
122.6	19.48±0.14	(1.60)
127.6	20.07±0.10	(1.63)
132.6	19.86±0.25	(1.66)
137.6	20.70±0.12	(1.69)
142.6	19.92±0.23	(1.66)
147.6	20.26±0.10	(1.65)
152.6	19.32±0.26	(1.63)
157.5	20.54±0.19	(1.70)
167.5	19.01±0.13	(1.55)
172.5	18.48±0.19	(1.53)
177.5	18.94±0.26	(1.60)
187.5	18.64±0.19	(1.54)
197.4	18.11±0.10	(1.48)
222.4	16.98±0.18	(1.41)
247.3	15.91±0.18	(1.32)
272.2	14.99±0.11	(1.23)
297.1	14.43±0.12	(1.19)
322.1	14.05±0.09	(1.15)
347.0	13.61±0.10	(1.12)
372.0	12.71±0.12	(1.05)
396.9	12.58±0.15	(1.05)
421.7	11.11±0.24	(0.99)
446.6	11.00±0.19	(0.95)
471.6	10.60±0.14	(0.89)

TABLE II. Absolute total cross sections for electron-impact single ionization of Kr^{5+}. The relative uncertainties are at the one-standard-deviation level; the absolute uncertainties (given in parentheses) are at a high confidence level corresponding to 90% confidence for the relative uncertainties.

E (eV)	σ (10^{-18} cm^2)	
48.7	−0.44±0.98	(1.67)
53.5	−0.24±0.58	(0.98)
58.7	0.53±0.82	(1.39)
63.5	0.45±0.54	(0.92)
68.2	0.57±0.57	(0.96)
73.5	0.37±0.38	(0.64)
75.6	0.82±0.55	(0.93)
77.7	1.37±0.22	(0.38)
79.6	0.37±0.39	(0.66)
81.4	0.59±0.44	(0.75)
82.2	3.05±0.52	(0.92)
83.6	3.70±0.28	(0.56)
86.1	7.59±0.57	(1.14)
88.0	6.75±0.25	(0.69)
89.9	8.12±0.57	(1.17)
92.2	7.76±0.57	(1.16)
93.7	7.65±0.32	(0.82)
96.0	9.24±0.47	(1.09)
98.0	9.30±0.14	(0.79)
102.6	10.52±0.23	(0.94)
107.6	9.87±0.52	(1.19)
112.6	11.75±0.58	(1.37)
117.6	10.40±0.35	(1.03)
122.6	11.79±0.64	(1.45)
127.7	11.92±0.38	(1.16)
132.7	11.70±0.87	(1.76)
137.6	12.19±0.24	(1.07)
142.7	12.80±0.81	(1.72)
147.6	12.37±0.33	(1.15)
152.7	13.20±0.59	(1.46)
157.6	12.72±0.19	(1.08)
162.5	13.25±0.40	(1.27)
167.6	13.61±0.49	(1.38)
172.6	13.43±0.48	(1.36)
177.6	13.82±0.43	(1.34)
182.5	13.18±0.15	(1.10)
187.5	14.02±0.50	(1.42)
192.5	13.80±0.48	(1.38)
197.5	13.81±0.29	(1.22)
222.4	13.79±0.22	(1.18)
247.3	14.04±0.39	(1.31)
272.2	13.89±0.55	(1.46)
297.1	14.29±0.38	(1.33)
322.1	13.64±0.44	(1.34)
347.1	13.39±0.37	(1.25)
372.0	13.46±0.34	(1.23)
396.9	13.40±0.22	(1.15)

mass electron-impact energy E, R is the product ion count rate, I_e, I_i, v_e, and v_i are the currents and velocities of the electrons and ions of charge qe, respectively, F is the form factor, and D is the detection efficiency, which was estimated [8] to be 98%.

B. Uncertainties

The relative uncertainties shown in Figs. 2–4 and in Tables I–III are at the one-standard-deviation level (1 s.d.) and are due to counting statistics only. The variation of the form factor during each measurement was negligible and thus is not included in the relative uncertainties. A quadrature sum of the absolute uncertainties of the measured quantities in Eq. (1), including the relative uncertainties (at a 90% confidence level, 1.7 s.d.) due to counting statistics, yields the total absolute uncertainty at a high confidence level for these measurements, also given in the tables. A detailed discussion of the absolute uncertainty can be found elsewhere [15]. The systematic uncertainties include: 4% from the absolute form factor, 4% from transmission of ions to the channeltron, 5% from signal ion detection and pulse transmission, 2% each from the measurement of the electron and ion currents, and 1% from the electron and ion velocities. As indicated in Tables I–III, the absolute uncertainties near the peak of the cross sections were typically 9%, 10%, and 12% for the Kr^{4+}, Kr^{5+}, and Kr^{7+} measurements, respectively.

TABLE III. Absolute total cross sections for electron-impact single ionization of Kr^+. The relative uncertainties are at the one-standard-deviation level; the absolute uncertainites (given in parentheses) are at a high confidence level corresponding to 90% confidence for the relative uncertainties.

E (eV)	σ (10^{-18} cm^2)	
117.9	0.23±0.36	(0.61)
124.0	1.01±0.55	(0.94)
126.2	0.71±0.33	(0.57)
127.9	0.69±0.33	(0.57)
130.1	1.08±0.37	(0.63)
132.4	0.92±0.36	(0.62)
134.0	1.24±0.33	(0.57)
137.9	2.03±0.38	(0.67)
142.9	3.21±0.47	(0.85)
147.9	3.95±0.21	(0.48)
152.9	4.35±0.36	(0.70)
157.8	4.95±0.32	(0.68)
162.8	5.55±0.48	(0.93)
167.8	5.42±0.33	(0.72)
172.8	5.34±0.23	(0.58)
177.3	5.65±0.44	(0.88)
177.8	5.36±0.37	(0.76)
178.9	6.03±0.45	(0.91)
181.1	6.29±0.42	(0.88)
182.8	6.72±0.27	(0.71)
187.8	6.07±0.33	(0.75)
192.8	6.53±0.34	(0.78)
197.7	6.33±0.21	(0.62)
207.7	6.43±0.29	(0.72)
222.7	6.92±0.34	(0.80)
227.6	6.74±0.25	(0.69)
247.5	7.13±0.21	(0.68)
272.5	7.88±0.32	(0.84)
297.4	7.34±0.20	(0.68)
347.2	7.88±0.20	(0.72)
397.1	8.61±0.11	(0.72)
446.8	8.68±0.30	(0.87)
496.6	8.54±0.20	(0.77)

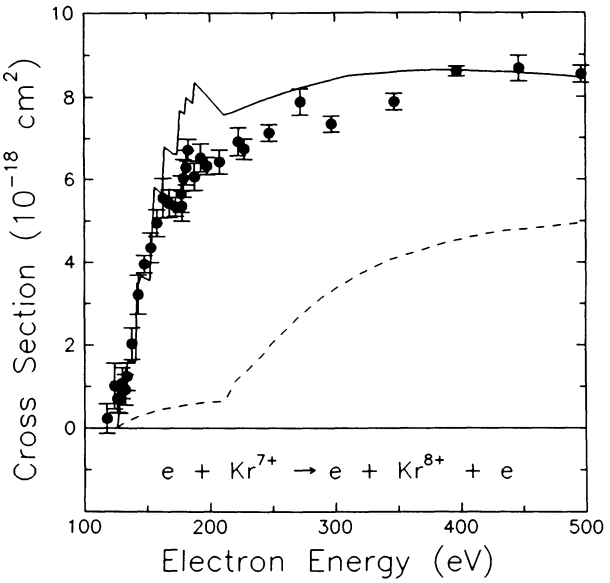

FIG. 4. Absolute cross sections as a function of electron-impact energy for single ionization of Kr^{7+}. The present experimental results are indicated by the solid circles with relative uncertainties at the one-standard-deviation level. The solid curve is a semirelativistic intermediate-coupled distorted-wave calculation and the dotted curve is a configuration-averaged distorted-wave calculation for direct ionization only (Ref. [14]).

III. RESULTS

Absolute total cross sections for electron-impact single ionization of Kr^{q+} ($q=4,5,7$) were measured from below threshold to 500 eV (400 eV for Kr^{5+}). The measurements were not extended beyond electron energies of 500 eV because of pressure loading of the apparatus at high electron energies and currents. The energy resolution of the electron gun is still uncertain because no sharp feature, such as a resonance, was found, but the resolution is expected to be 0.5 eV full width at half maximum or less. The results for the three charge states of krypton studied are presented below in separate sections.

A. Kr^{4+}

Absolute cross sections for single ionization of Kr^{4+} ions by electrons are shown in Fig. 2. The error bars represent relative uncertainties only, at the one-standard-deviation level (1 s.d.). The data are also given in Table I, with relative uncertainties at 1 s.d. and abso-

lute uncertainties at a high confidence level (see discussion of uncertainties above). The curves in Fig. 2 are the results of configuration-average distorted-wave (CADW) calculations for direct ionization only (dotted curve) and for direct ionization plus excitation-autoionization (solid curve) for the $4s^24p^2$ ground configuration [14]. Excitations were included for $3d \rightarrow nl$ ($n=4,5,6$) and $4s \rightarrow 6l$ transitions. The configuration-average energy levels, calculated with Cowan's relativistic Hartree-Fock (HFR) code [19], are given in Ref. 14, along with those of the other relevant charge states of krypton.

One set of Kr^{4+} data points, with electron energies ranging from 28.5 to 97.6 eV, showed a monotonic increase of cross section with decreasing energy below 50 eV, indicative of spurious beam effects. This data set was corrected by subtracting a least-squares fit curve of the form AE^{-2} (with $A=3.59\times10^{-15}$ cm^2 eV^2) and then was averaged with the other Kr^{4+} data sets. The measured cross sections below 50 eV are zero within the experimental uncertainties. The nonzero cross sections from about 50 eV to the ground-state ionization threshold [20] of 64.7 eV indicate the presence of metastable ions in the Kr^{4+} beam, possibly in the $4s4p^3$ configuration which lies 16.2 eV above the ground state [20]. Assuming a metastable threshold of 48.5 eV, the point at 63.4 eV, just below the ground-state threshold, corresponds, to an energy of 1.31 threshold units. Using the assumption that the ionization cross section is essentially the same from the ground and metastable configurations when the energy is expressed in threshold units, we estimate that the metastable fraction of the Kr^{4+} ion beam was 0.076 ± 0.030.

The measured cross sections are in good agreement with the CADW calculations for the ionization of the Kr^{4+} ground configuration, particularly above 125 eV and since about 10% of the cross section appears to be from metastable ions. In the region between the ground-state threshold and 125 eV, where the largest contributions from excitation-autoionization occur, the measured cross sections are significantly larger than the CADW predictions, although the difference is less than 15% above 110 eV.

B. Kr^{5+}

Figure 3 shows the measured absolute total cross sections for electron-impact single ionization of Kr^{5+} from below threshold to 400 eV, with the error bars representing 1 s.d. relative uncertainties only. The data are also given in Table II, with relative uncertainties at 1 s.d. and absolute uncertainties at a high confidence level (see discussion of uncertainties above). The curves in Fig. 3 are the results of CADW calculations for direct ionization only (dotted curve) and for direct ionization plus excitation-autoionization (solid curve) for the $4s^24p$ ground configuration [14]. The energy levels for the excitations included, as calculated with Cowan's HFR code [19], are given in Ref. [14].

Nonzero cross sections between 60 eV and the ground-state ionization threshold [20] of 78.5 eV indicate Kr^{5+} ions in a metastable configuration, most likely a $4s4p^2$ configuration whose configuration-average energy is 13.98 eV above the ground state. Taking the metastable ionization threshold to be 64.5 eV and making the assumptions used for estimating the Kr^{4+} ion beam metastable fraction, we calculate that the metastable fraction was 0.163 ± 0.037 for the Kr^{5+} ion beam.

For electron energies above 125 eV, the measured cross sections for ionization of Kr^{5+} are in excellent agreement with the CADW predictions. However, as for the Kr^{4+} case, the measured cross sections between the ground-state threshold and 125 eV are consistently higher than the CADW calculations.

C. Kr^{7+}

Measured absolute total cross sections for electron-impact single ionization of Kr^{7+} are plotted in Fig. 4, with the error bars representing 1 s.d. relative uncertainties only. Table III gives the measured data along with absolute uncertainties at a high confidence level (equivalent to 90% confidence level for the relative uncertainties). The dotted curve in Fig. 4 is a CADW calculation for direct ionization of the $3d^{10}4s$ ground configuration. The solid curve is a semirelativistic intermediate-coupled distorted-wave (DWIC) calculation including both term dependence and relaxation effects [14]. As a guide, configuration-average energies (*LS* coupling) calculated with the HFR code [19] are also given in Ref. [14].

The zero cross section below the ground-state threshold [20] of 125.8 eV indicates an absence of metastables in the Kr^{7+} beam. Excellent agreement exists between the measured cross sections and the theoretical predictions, from the ionization threshold up to 500 eV. The largest difference between the two is about 15% near 190 eV, although the difference is much smaller over most of the measured energy range. When contrasted with the results of the Kr^{4+} and Kr^{5+} cases, the improved agreement achieved for the Kr^{7+} ions emphasizes the need for term-dependent calculations in order to predict the contribution of excitation-autoionization to the total cross section near threshold.

Although no sharp feature such as a resonance was found, an upper limit of 2.5 eV for the electron energy resolution for the electrostatic gun can be inferred from the measured excitation onset near 178 eV.

IV. SUMMARY

Absolute total cross sections for electron-impact single ionization of Kr^{q+} ($q=4,5,7$) ions were measured using the ORNL crossed-beams apparatus, with absolute uncertainties of 12% or less. The measurements agree well with distorted-wave calculations detailed in the following paper, although there are some discrepancies near threshold for the configuration-average calculations done for the Kr^{4+} and Kr^{5+} cases. Agreement was greatly improved by the term-dependent calculations used for Kr^{7+}. Metastable fractions of 0.076 ± 0.030 and 0.163 ± 0.037 were estimated for the Kr^{4+} and Kr^{5+} ion beams, respectively. An absence of metastables was inferred for the Kr^{7+} ion beam. The ionization cross sec-

tions for all three ions showed significant contributions from excitation-autoionization, particularly near threshold, as expected from published results on the xenon isonuclear sequence [13].

ACKNOWLEDGMENTS

The authors wish to thank D. C. Gregory, G. H. Dunn, E. W. Bell, A. C. H. Smith, F. W. Meyer, and C. C. Havener for valuable discussions and J. W. Hale for skilled technical assistance. We are grateful to T. W. Gorczyca, M. S. Pindzola, N. R. Badnell, and D. C Griffin for providing us with results of their calculations prior to publication. This work was supported by the Division of Applied Plasma Physics, Office of Fusion Energy of the U.S. Department of Energy under Contract No. DE-AC05-84OR21400 with Martin Marietta Energy Systems, Inc., and Contract No. DE-A105-86ER532237 with the National Institute of Standards and Technology. M.E.B. acknowledges an appointment to the ORNL Postdoctoral Research Associates Program administered jointly by ORNL and Oak Ridge Associated Universities.

[1] R. K. Janev, M. F. A. Harrison, and H. W. Drawin, Nucl. Fusion **29**, 109 (1989).
[2] G. H. Dunn, Nucl. Fusion Suppl. At. Plasma Mater. Interaction Data Fusion **2**, 25 (1993).
[3] IAEA Summary Report No. INDC(NDS)-277, 1993 (unpublished).
[4] D. C. Gregory, Nucl. Instrum. Methods Phys. Res. B **10-11**, 87 (1985).
[5] K. Tinschert, A. Müller, G. Hofmann, C. Achenbach, R. Becker, and E. Salzborn, J. Phys. B **20**, 1121 (1987).
[6] A. Matsumoto, A. Danjo, S. Ohtani, H. Suzuki, H. Tawara, T. Takayanagi, K. Wakiya, I. Yamada, M. Yoshino, and T. Hirayama, J. Phys. Soc. Jpn. **59**, 902 (1990).
[7] H. Lebius, H. R. Koslowski, K. Wiesemann, and B. A. Hüber, Ann. Phys. (Leipzig) **48**, 103 (1991).
[8] D. C. Gregory, P. F. Dittner, and D. H. Crandall, Phys. Rev. A **27**, 724 (1983).
[9] M. E. Bannister, D. W. Mueller, L. J. Wang, M. S. Pindzola, D. C. Griffin, and D. C. Gregory, Phys. Rev. A **38**, 38 (1988).
[10] M. S. Pindzola, D. C. Griffin, C. Bottcher, D. H. Crandall, R. A. Phaneuf, and D. C. Gregory, Phys. Rev. A **29**, 1749 (1984).
[11] K. Tinschert, A. Müller, R. Becker, and E. Salzborn, J. Phys. B **20**, 1823 (1987).
[12] W. T. Rogers, G. Stefani, R. Camilloni, G. H. Dunn, A. Z. Msezane, and R. J. W. Henry, Phys. Rev. A **25**, 737 (1982).
[13] D. C. Griffin, C. Bottcher, M. S. Pindzola, S. M. Younger, D. C. Gregory, and D. H. Crandall, Phys. Rev. A **29**, 1729 (1984).
[14] T. W. Gorczyca, M. S. Pindzola, N. R. Badnell, and D. C. Griffin, following paper, Phys. Rev. A **49**, 4682 (1994).
[15] D. C. Gregory, F. W. Meyer, A. Müller, and P. Defrance, Phys. Rev. A **34**, 3657 (1986).
[16] P. O. Taylor, K. T. Dolder, W. E. Kauppila, and G. H. Dunn, Rev. Sci. Instrum. **45**, 538 (1974).
[17] G. H. Dunn and B. Van Zyl, Phys. Rev. **154**, 40 (1967).
[18] See, for example, M. F. A. Harrison, Br. J. Appl. Phys. **17**, 371 (1966).
[19] R. D. Cowan, *The Theory of Atomic Structure and Spectra* (University of California, Berkeley, 1981).
[20] J. Sugar and A. Musgrove, J. Chem. Phys. Ref. Data **20**, 859 (1991).